Electrostatic Sample-Tip Interactions in the Scanning Tunneling Microscope

M. McEllistrem, G. Haase, D. Chen, and R. J. Hamers[(a)]

Department of Chemistry, University of Wisconsin-Madison, 1101 University Avenue, Madison, Wisconsin 53706

(Received 3 August 1992)

Local surface photovoltage (SPV) measurements were used to measure how the electric field of a scanning tunneling microscope tip perturbs the electronic band structure at Si(001), Si(111)-(7×7), and H-terminated Si(111) surfaces. The results demonstrate that tip-induced band bending is important under typical STM conditions even on surfaces whose surface Fermi levels are nominally "pinned." Spatially resolved measurements of band bending as a function of sample bias show that atomic-scale contrast in SPV images can result from local variations in the ability of the surface states under the tip to screen external electric fields.

PACS numbers: 73.20.At, 61.16.Ch, 72.40.+w, 73.50.Pz

Recent advances in the use of the scanning tunneling microscope (STM) as a tool for atomic-scale characterization of surface geometry and electronic structure [1-3] and as an active tool for atomic-scale manipulation on semiconductor surfaces [4,5] have underscored the importance of understanding the electrostatics at *atomic-sized* tunnel junctions. One often asked question is whether the tip is a nonintrusive probe, or whether the high electric field at the tip affects the electronic structure of the sample. STM and tunneling spectroscopy studies virtually always assume that the sample-tip bias is dropped between the tip and the *surface* of the sample, and is therefore a valid energy scale for tunneling spectroscopy [1,2,6]. However, Feenstra and Stroscio [3] and others [7,8] have pointed out that on semiconductors the electric field from the STM tip might penetrate into the bulk. This sample-tip interaction cannot be readily predicted because it depends on the local surface electronic structure and the shape of the tip, nor can it be measured using conventional tunneling spectroscopy techniques. However, penetration of the tip electric field beneath the semiconductor surface *can* be measured using the STM tip as a probe of the local surface photovoltage (SPV) [9]. Here, we present the first measurements *quantitatively* demonstrating how the STM tip perturbs the subsurface electronic structure of semiconductors under typical STM operating conditions; we also show that this perturbation is controlled by the *local* surface state density and hence can vary on atomic distance scales.

Sub-surface electric fields from the STM tip or from charged surface states will cause the conduction and valence bands of a semiconductor to "bend" by an amount V_{BB}. Excess electrons and holes produced by illumination will be separated by these fields, giving rise to a potential difference between the surface and bulk: the surface photovoltage. The sign of the SPV reveals the direction of band bending; its magnitude depends on V_{BB}, the carrier recombination rate, and the light intensity. At sufficiently high intensities, a "flat band" condition is achieved in which $V_{SPV}=V_{BB}$. For a given surface at any fixed intensity, however, the SPV is a direct measure of V_{BB}.

We measure the SPV using an ac potentiometry method that works over a wide range of biases and tunneling currents (I_{tunnel}). Light from a 5 mW HeNe laser (632.8 nm) is chopped at 4 kHz and impinges on the STM junction at 79° from the tip axis. Chopping the light beam [represented by $f(t)$, where $f(t)=0$ or 1] produces a modulated photovoltage $V_{SPV}f(t)$. The sample bias consists of a dc component V_{samp} with a unipolar modulation $V_{mod}f(t)$ synchronized with the chopper. An integrating feedback system adjusts the sign and magnitude of V_{mod} such that I_{tunnel} [and therefore also the total surface potential $V_{surface}=V_{samp}+V_{mod}f(t)+V_{SPV}f(t)$] remains constant. Numerical calculations [10] show that at moderate illumination intensities direct tunneling of photoexcited carriers is negligible and the only significant effect of illumination is a change in surface potential. They also show that for nondegenerate semiconductors the tunneling electrons originate within 5 Å of the surface, so that I_{tunnel} is uniquely determined by the *surface* potential $V_{surface}$ and tunneling experiments as described here quantitatively measure the SPV. All measurements were made in ultrahigh vacuum (UHV). Atomic resolution was routinely achieved on all surfaces and barrier height measurements showed heights of 3-4 eV, demonstrating that measurements were made in the vacuum tunneling, rather than point-contact, regime. The samples were *n*- and *p*-type Si(001), 0.10±0.02 Ω cm, and Si(111), 0.12±0.02 Ω cm. Si(111)-(7×7) and Si(001)-(2×1) were prepared by annealing to 1150 °C. Hydrogen-terminated Si(111) [Si(111)-H] was prepared by dipping Si(111) into HF/NH_4F solutions [11] and immediately introducing into UHV.

Here we report experiments on three prototypical surfaces. The Si(111)-(7×7) surface has a very high local density of states (LDOS) throughout the gap which strongly pins the Fermi level near midgap [2]. Si(001)-(2×1) has a surface-state band gap, but the Fermi level is pinned locally by surface defects [12]. Si(111)-H has no surface states in the gap and the Fermi level is unpinned [11]. We therefore expect that the SPV should be >0 for *n*-type and <0 for *p*-type samples of Si(111)-(7×7) and Si(001), but should be approximately zero for

© 1993 The American Physical Society

H-Si(111), in the absence of external fields.

Figure 1 shows how the SPV varies as a function of applied bias. These measurements were made by stopping the tip raster during image acquisition, ramping the voltage up and down while measuring SPV and the "topography" data (hopping over the range near zero bias), and then continuing the image acquisition, while maintaining a constant I_{tunnel} of 0.3 nA. Because the sample-tip separation changes slightly (typically ≈ 1 Å) during the voltage scan the electric field varies slightly more slowly than the applied voltage. The topography data and barrier height measurements confirm that the STM remains in the vacuum tunneling regime. In Fig. 1, several features are immediately apparent. First, the SPV is strongly dependent on V_{samp} for Si(111)-H and Si(001)-(2×1), but is nearly independent of V_{samp} for Si(111)-(7×7). Second, at low bias all curves tend toward $V_{\text{SPV}}>0$ for n-type and $V_{\text{SPV}}<0$ for p-type samples, in agreement with the above predictions. Finally, in some cases the sign of the SPV can invert depending on the applied bias.

The results in Fig. 1 demonstrate that on Si(111)-H, the electric field from the STM tip penetrates substantially into the subsurface region, where it induces a band bending V_{BB}. Because this surface has no surface states, the tip can bend the bands until one of the band edges intersects the Fermi level, at which point the SPV saturates as depicted in Figs. 2(a) and 2(b) for an n-type sample. Experimentally, Fig. 1 shows that the SPV saturates at -0.11 ± 0.04 V for $V_{\text{samp}}\ll 0$ and $+0.8\pm0.1$ V for $V_{\text{samp}}\gg 0$, in good agreement with the values of -0.15 ± 0.03 V and $+0.97\pm0.03$ V calculated from the bulk band gap and E_F of our samples (0.15 ± 0.03 eV beneath the bulk conduction band minimum). This agreement, and the insensitivity of the measured SPV to intensity, leads us to conclude that we have achieved flat band conditions where $V_{\text{SPV}}=V_{\text{BB}}$ (more generally, $V_{\text{SPV}}\leq V_{\text{BB}}$). We then conclude from Fig. 1 that with a 1.5 V bias, for example, the tip field *enhances* the nascent band bending by at least 0.4 V, and at least 25% of the 1.5 V sample-tip potential difference is dropped within the semiconductor. To confirm these observations, we have numerically solved Poisson's equation for the three-dimensional geometry of a parabolic tip ($z=20+r^2/r_0^2$, with r, r_0, and z in Å and $r_0=500$) ending in a sphere of radius 10 Å with the tip end 10 Å from a 2×10^{17} cm^{-3} n-type silicon surface; as shown in Fig. 1, these calculations predict tip-induced band bending in good agreement with our observations for Si(111)-H. Other calculations show that the band bending depends on the detailed tip shape, but the results in Fig. 1 are typical for the tip sizes and shapes used in STM. Large tip-induced band bending should be a general characteristic of semiconductors with wide surface state band gaps, and is further supported by additional experimental measurements on GaAs(110).

We now consider the effect of adding gap states which can pin the Fermi level, as typified by Si(001)-(2×1). The (2×1) reconstruction produces a filled π state and an empty π^* state located at 0.2 eV below the valence band maximum (VBM) and 0.4 eV below the conduction band minimum (CBM), respectively [13], and constrains E_F at the surface between the VBM and the empty π^* state. Additionally, surface defects at a density of $\sim10^{13}$ cm^{-2} give rise to a narrow defect state $\sim$0.1 eV wide at E_F. While this defect density is orders of magnitude higher than the 10^{10}–10^{11} cm^{-2} needed to globally pin E_F midgap, Fig. 1 shows that electric field from the tip locally unpins the surface. At $V_{\text{samp}}>0$ the field from the tip

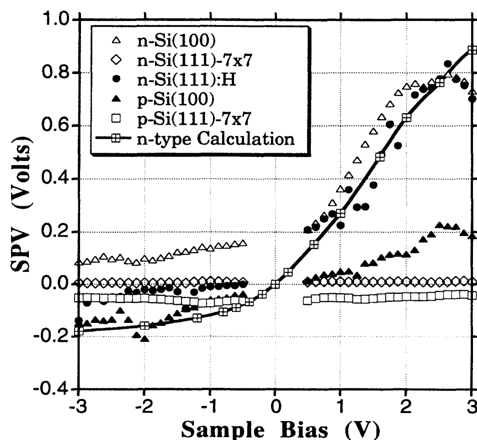

FIG. 1. Surface photovoltage vs V_{samp} at 0.3 nA tunneling current for n- and p-type Si(001)-(2×1), Si(111)-7×7, and for H-terminated Si(111) surfaces.

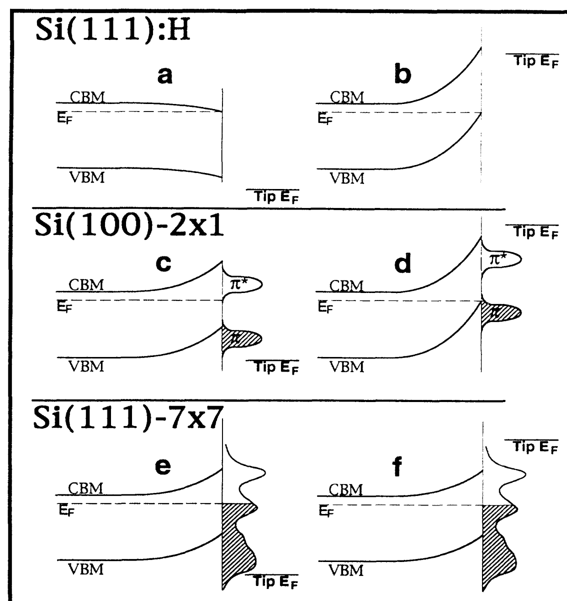

FIG. 2. Schematic illustration of tip-induced band bending for n-type H-terminated Si(111) [(a),(b)], Si(001)-(2×1) [(c),(d)], and Si(111)-7×7 [(e),(f)] for $V_{\text{samp}}\ll 0$ [(a),(c),(e)] and $V_{\text{samp}}\gg 0$ [(b),(d),(f)].

bends the bands up until the Fermi level meets the VBM, giving rise to a maximum SPV of $+0.8 \pm 0.1$ V compared with the maximum anticipated value of $+0.97 \pm 0.03$ V [Fig. 2(d)]. For $V_{samp} \leq 0$ the bands remain bent up because at the surface E_F becomes pinned at the bottom of the empty π^* state [Fig. 2(c)], reaching a value of $+0.09 \pm 0.03$ V (Fig. 1). Figure 1 shows that on *p*-type samples, tip-induced band bending gives rise to SPV's ranging between $+0.18 \pm 0.05$ V for $V_{samp} \gg 0$ (in agreement with the $+0.10 \pm 0.03$ V anticipated from $E_F - E_{VBM}$) and -0.15 ± 0.05 V for $V_{samp} \ll 0$ (when E_F again meets the bottom of the empty π^* state).

Finally, we consider the Si(111)-(7×7) surface. Figure 1 shows that on Si(111)-(7×7) the SPV is always positive on the *n*-type and negative on the *p*-type sample, and is nearly *independent* of V_{samp}. The insensitivity of SPV to V_{samp} demonstrates that the field from the tip does not penetrate the surface to any substantial extent because the surface states at E_F screen external fields. While on Si(001) and Si(111)-H the SPV is large and nearly independent of intensity, corresponding to illuminated flat band conditions where $V_{SPV} = V_{BB}$, Fig. 1 shows that for Si(111)-(7×7) under identical conditions the SPV is small: only $+0.01 \pm 0.01$ V for *n*-type and -0.06 ± 0.02 V for the *p*-type samples, compared with a maximum of ± 0.45 V anticipated for midgap pinning. The ability to achieve flat band conditions by illuminating Si(001)-(2×1) and Si(111)-H but not Si(111)-(7×7) arises from the latter's high rate of surface recombination, which in turn is directly correlated with its high density of surface states. Quantitative measurement of the flat band SPV on this unusual surface requires prohibitively intense illumination [14,15].

The results in Fig. 1 show two important facts: First, that tip-induced band bending is important over the range of conditions typically used for STM and tunneling spectroscopy (STS) measurements, and second, that the field from the tip can locally unpin the Fermi level even on surfaces which, based on macroscopic considerations, have "pinned" Fermi levels. These results have important implications for STS measurements [1,2,6]. While STS measurements on Si(111)-(7×7) showed surface states agreeing with those observed using photoelectron spectroscopies [2], STS measurements on other silicon surfaces [12,16] and other semiconductors [16,17] generally show anomalously large band gaps. The agreement for Si(111)-(7×7) arises because of its "metallic" density of states at E_F. For surfaces with lower LDOS at E_F, only part of the sample-tip potential will be dropped between the tip and *surface*, and STS measurements will in general be in error (measuring gaps too large) and will be irreproducible due to changes in the tip shape. While tip-induced band bending can be estimated by fitting STS data *if* the local surface electronic structure is already known [3], in the more general case this is not possible because neither the surface LDOS nor the detailed shape of the tip are known independently. Local SPV measurements provide a way of measuring the tip-induced band bending and correcting the STS energy scale.

Because the amount of tip-induced band bending is dependent on the local surface electronic structure, it also varies across the surface. Figure 3(a) shows an STM topograph ($V_{samp} = +2.0$ V) of *p*-type Si(111)-(7×7) after exposure to 0.1 L (1 L = 1×10^{-6} Torr s) at 300 K, while

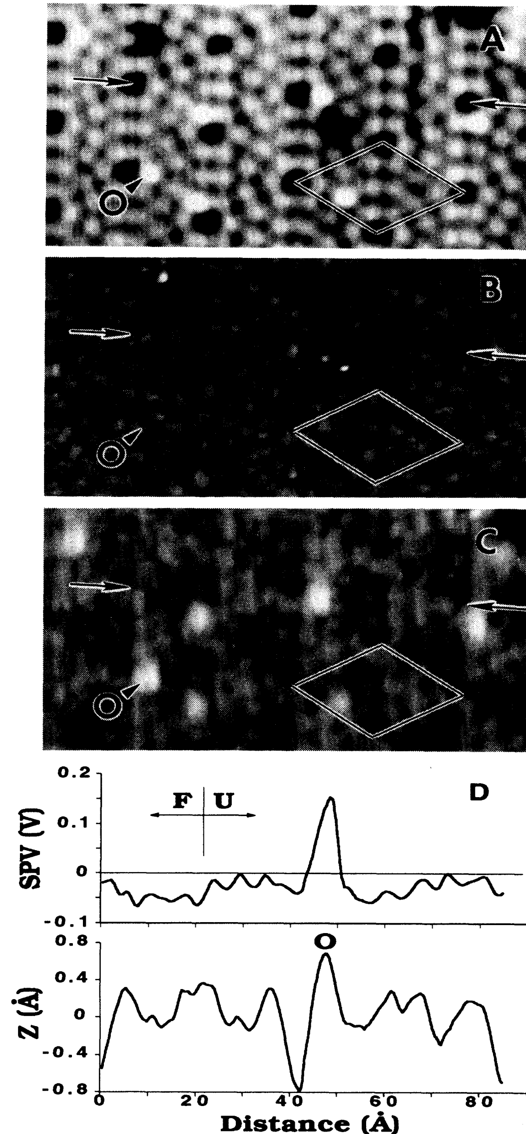

FIG. 3. Topography and spatial distribution of surface photovoltage; images were taken simultaneously on *p*-Si(111)-(7×7) after exposure to ~0.1 L O_2 at 300 K. "O" indicates an oxygen atom. One (7×7) unit cell is outlined. (a) Topography at $V_{samp} = +2.0$ V. (b) Spatial distribution of SPV at $V_{samp} = +0.5$ V. (c) Spatial distribution of SPV at $V_{samp} = +2.0$ V. (d) Line scan of topography and SPV measured between the arrows indicated in (a) and (c). "F" and "U" indicate faulted and unfaulted halves of the unit cell.

Figs. 3(b) and 3(c) show spatial maps of the SPV measured with $V_{samp}=+0.5$ and $+2.0$ V, respectively. All images were acquired simultaneously, alternating between two values of V_{samp} on successive lines but with a constant $I_{tunnel}=200$ pA. In Fig. 3(a), the bright protrusions (labeled "O") correspond to chemisorbed oxygen atoms, which open a gap in the local density of states [18,19]. For $V_{samp}=+0.5$ V [Fig. 3(b)] the SPV image is nearly featureless with an average value of -70 mV. At $V_{samp}=+2.0$ V [Fig. 3(c)], however, the SPV image shows clear atomic-scale variations which can be seen more quantitatively in Fig. 3(d). While over most of the surface the SPV is still negative, when the tip is over the oxygen atoms the SPV even inverts to a value of $+0.11\pm0.05$ V. The SPV contrast observed at other adsorbates or defects depends on their LDOS near E_F.

While electrostatic considerations suggest that the *intrinsic* surface band bending should vary only on length scales of (typically) hundreds of angstroms, the presence [9,15,20,21] or absence [22,23] of atomic-scale spatial contrast in STM-SPV measurements has been controversial. Proposed contrast mechanisms include spatial variations in the subsurface band bending and rate of surface recombination [9], the efficiency of optical rectification [15], experimental artifacts [23], and charging effects [21]. Cahill and Hamers [21] showed that at high tunneling currents charge trapping can induce an atomically varying SPV; however, we use 20-fold higher conductivity samples than Cahill and Hamers and very low currents; we find that charging is then eliminated, but the field effect remains important. Moreover, the contrast in Figs. 3(b) and 3(c) cannot arise from current-induced charging since the two SPV images were taken at the *same* I_{tunnel}; rather, the contrast arises from the fact that oxygen atoms reduce the local density of states at E_F, making it possible for the electric field at the tip to *locally* induce an upward band bending, which we then detect through the SPV. The observed SPV of $+0.11$ V at the oxygen atoms is in good agreement with the maximum SPV of 0.10 ± 0.03 V anticipated when the valence band meets the Fermi level.

Careful examination of Figs. 3(c) and 3(d) also shows that at 2 V bias the "faulted" and "unfaulted" halves of the unit cell have different average SPV's of -60 ± 10 mV and -20 ± 10 mV, respectively. This contrast does not exist in the SPV image taken with $V_{samp}=+0.5$ V [Fig. 3(b)], nor can it be explained by the contour that the tip follows since at $V_{samp}=+2.0$ V the two halves are indistinguishable in the topograph. In agreement with previous results which show a higher state density at E_F in the faulted than in the unfaulted half, Fig. 3(c) shows that the faulted half can better screen the electric field and hence shows less tip-induced band bending.

In conclusion, we have performed the first direct quantitative measurements showing how the *local* electric field of the tip perturbs the electronic structure of semiconductors. Our results show that while the degree of tip-induced band bending is controlled by the surface states, even surfaces which are pinned by defects such as Si(001) can be unpinned by the tip, leading to possible errors in tunneling spectroscopy measurements. Finally, we find that tip-induced band bending can give rise to atomic resolution in spatial maps of the SPV, with contrast arising from the local degree of Fermi-level pinning.

This work was supported in part by the U.S. Office of Naval Research and the Camille and Henry Dreyfus Foundation.

[a] Author to whom correspondence should be addressed.

[1] R. S. Becker *et al.*, Phys. Rev. Lett. **55**, 2032 (1985).
[2] R. J. Hamers, R. M. Tromp, and J. E. Demuth, Phys. Rev. Lett. **56**, 1972 (1986).
[3] R. M. Feenstra and J. A. Stroscio, J. Vac. Sci. Technol. B **5**, 923 (1987).
[4] I. Lyo and P. Avouris, Science **253**, 173 (1991).
[5] J. A. Stroscio and D. M. Eigler, Science **254**, 1319 (1991).
[6] R. M. Feenstra, J. A. Stroscio, and A. P. Fein, Surf. Sci. **181**, 295 (1987).
[7] W. J. Kaiser *et al.*, J. Vac. Sci. Technol. A **6**, 519 (1988).
[8] M. Weimer, J. Kramar, and J. D. Baldeschwieler, Phys. Rev. B **39**, 5572 (1989).
[9] R. J. Hamers and K. Markert, J. Vac. Sci. Technol. A **8**, 3524 (1990).
[10] M. T. McEllistrem and R. J. Hamers (to be published).
[11] G. S. Higashi *et al.*, Appl. Phys. Lett. **56**, 656 (1990).
[12] R. J. Hamers and U. K. Köhler, J. Vac. Sci. Technol. A **7**, 2854 (1989).
[13] F. J. Himpsel and T. Fauster, J. Vac. Sci. Technol. A **2**, 815 (1984).
[14] R. J. Hamers and K. Markert, Phys. Rev. Lett. **64**, 1051 (1990).
[15] Y. Kuk *et al.*, Phys. Rev. Lett. **65**, 456 (1990).
[16] R. M. Feenstra, Phys. Rev. B **44**, 13791 (1991).
[17] L. J. Whitman *et al.*, Phys. Rev. B **44**, 5951 (1991).
[18] I. W. Lyo *et al.*, J. Phys. Chem. **94**, 4400 (1990).
[19] J. P. Pelz and R. H. Koch, Phys. Rev. B **42**, 3761 (1990).
[20] Y. Kuk *et al.*, J. Vac. Sci. Technol. **9**, 545 (1991).
[21] D. G. Cahill and R. J. Hamers, J. Vac. Sci. Technol. B **9**, 564 (1991).
[22] D. G. Cahill and R. J. Hamers, Phys. Rev. B **44**, 1387 (1991).
[23] G. P. Kochanski and R. F. Bell, Surf. Sci. **273**, L435 (1992).

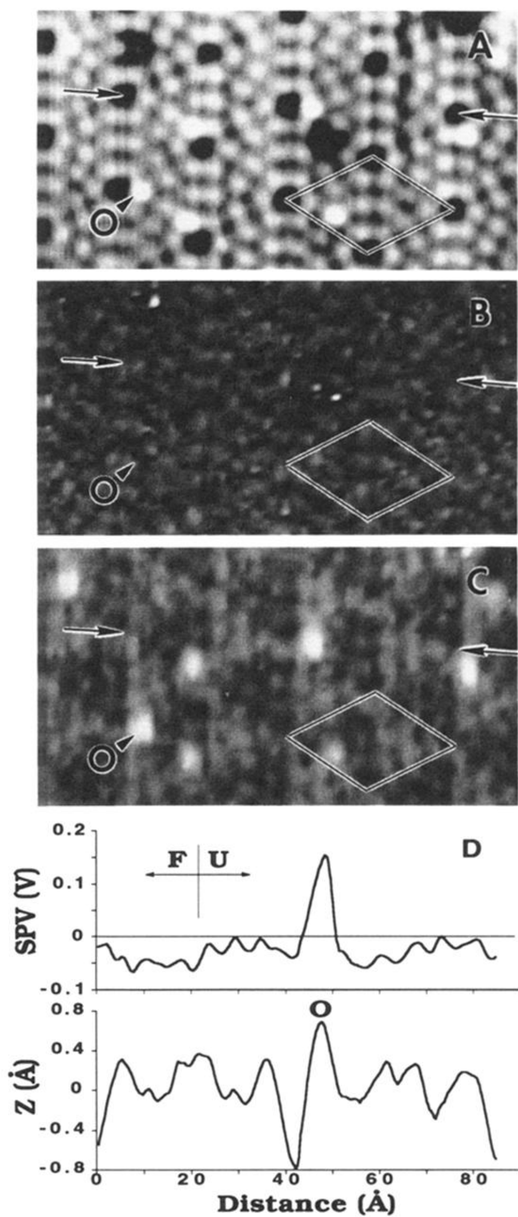

FIG. 3. Topography and spatial distribution of surface photovoltage; images were taken simultaneously on p-Si(111)-(7×7) after exposure to ∼0.1 L O_2 at 300 K. "O" indicates an oxygen atom. One (7×7) unit cell is outlined. (a) Topography at $V_{samp}=+2.0$ V. (b) Spatial distribution of SPV at $V_{samp}=+0.5$ V. (c) Spatial distribution of SPV at $V_{samp}=+2.0$ V. (d) Line scan of topography and SPV measured between the arrows indicated in (a) and (c). "F" and "U" indicate faulted and unfaulted halves of the unit cell.